Discover Chemistry

Research

Computational design and molecular insights into acetylcholinesterase inhibitors from *Aristolochia indica* for Alzheimer's disease therapy

Srinivasarao Mande[1] · Lalitha Repudi[1] · Sanchari Goswami[1] · Nadia Psalms Gangavarapu[1] · Hamid Ghaffoori Hasan[2] · Kumaraswamy Gandla[1]

Received: 24 November 2024 / Accepted: 5 May 2025

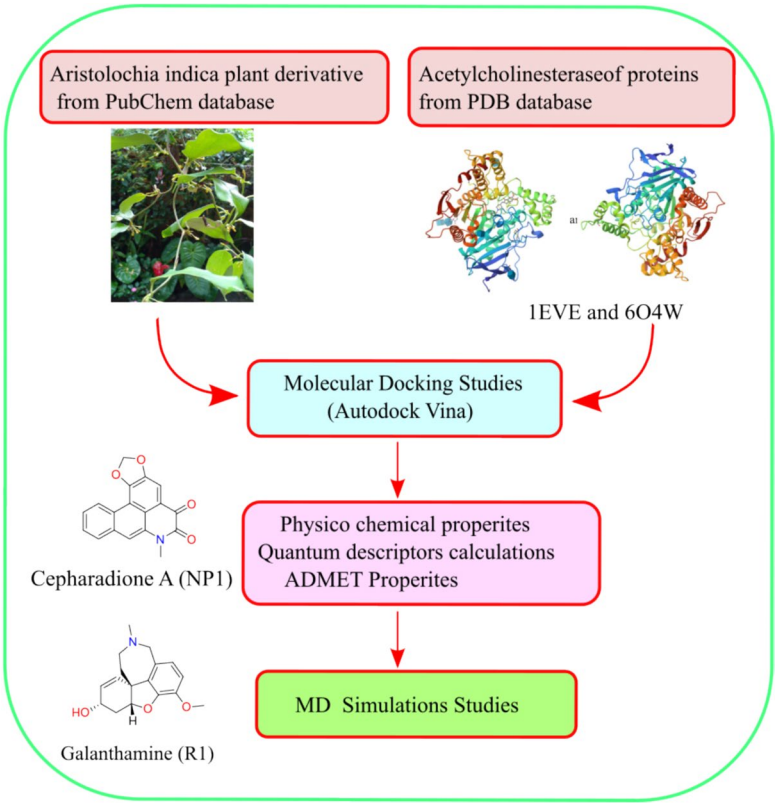
Published online: 24 May 2025
© The Author(s) 2025, corrected publication 2025 OPEN

Abstract

Alzheimer's disease (AD) remains a major neurodegenerative disorder with limited effective treatments, necessitating the search for novel acetylcholinesterase (AChE) inhibitors to mitigate cognitive decline. While synthetic inhibitors pose concerns regarding toxicity and bioavailability, natural compounds from *Aristolochia indica* present a promising yet underexplored alternative. This study employed molecular docking, molecular dynamics (MD) simulations, and in silico drug-likeness and ADME profiling to evaluate fourteen bioactive compounds against human AChE (hAChE, PDB: 6O4W) and Torpedo californica AChE (TcAChE, PDB: 1EVE). Docking analysis revealed binding affinities ranging from − 8.2 to − 11.2 kcal/mol (hAChE) and − 8.1 to − 11.2 kcal/mol (TcAChE), with Cepharadione A (NP1) exhibiting the highest affinity (− 11.2 kcal/mol) via multiple stabilizing interactions within the active site. MD simulations confirmed the structural stability of NP1, NP2 (Savinin), and NP3 (Aristolactam II) complexes, with RMSD < 2.0 Å over 100 ns. Drug-likeness and ADME evaluations indicated favorable pharmacokinetic properties, including optimal lipophilicity (LogP 1.84–5.0), high gastrointestinal absorption, and blood–brain barrier permeability. Most compounds demonstrated minimal P-glycoprotein efflux and selective metabolism via cytochrome P450 enzymes, supporting their CNS drug potential. Quantum chemical calculations further corroborated electronic stability and reactivity. These findings highlight *A. indica*-derived compounds as promising AChE inhibitors, addressing the need for safer and more effective natural alternatives for AD therapeutics and warranting further experimental validation.

✉ Kumaraswamy Gandla, drkumaraswamygandla@gmail.com; Srinivasarao Mande, drsrinivasaraomande@gmail.com; Lalitha Repudi, repudilalitha@gmail.com; Sanchari Goswami, sancharig89@gmail.com; Nadia Psalms Gangavarapu, npg9495@gmail.com; Hamid Ghaffoori Hasan, hamid@uomanara.edu.iq | [1]Department of Pharmacy, Chaitanya (Deemed to be University), Gandipet, Himayatnagar (Village), Moinabad (Mandal), Hyderabad 500075, Telangana, India. [2]Pharmacy Department, Al-Manara College of Medical Sciences, Maysan, Iraq.

Graphical Abstract



Keywords Natural compounds · Alzheimer's disease · Drug-likeness · Molecular docking · Molecular dynamics simulations · Quantum calculations

1 Background

Alzheimer's disease (AD) remains the most prevalent form of dementia, characterized by a progressive decline in cognitive abilities, coupled with behavioral and neuropsychiatric disturbances [1]. Recent global estimates indicate that approximately 35 million individuals are living with AD. Projections suggest a substantial rise in prevalence, reaching 65 million by 2030 and 115 million by 2050. These alarming statistics emphasize the urgent need for the development of effective therapeutic interventions [2]. Acetylcholinesterase is a key enzyme in the hydrolysis of acetylcholine, a critical neurotransmitter involved in cognitive function. By catalyzing the breakdown of acetylcholine in the synaptic cleft, acetylcholinesterase plays a pivotal role in regulating cholinergic signaling, which is essential for the proper transmission of nerve impulses and the termination of synaptic activity [3]. The hydrolysis process, converting acetylcholine into choline and acetic acid, is integral to maintaining homeostasis in neurotransmission. However, in AD, dysregulation of acetylcholine metabolism contributes to cognitive deficits. Specifically, the depletion of acetylcholine, exacerbated by the unchecked activity of acetylcholinesterase, is a hallmark of AD pathology [4].

To mitigate the effects of acetylcholine depletion, several pharmacological agents have been developed. Currently approved medications such as donepezil, rivastigmine, and galantamine function as acetylcholinesterase inhibitors, thereby increasing acetylcholine concentrations in the synaptic cleft. While these drugs provide symptomatic relief, they are not without limitations, as they are frequently associated with adverse effects. This underscores the pressing need for novel and more effective therapeutic strategies to address the complex pathophysiology of AD and to improve patient outcomes [5, 6].

Computer-aided drug design (CADD) plays a crucial role in the discovery and development of therapeutic agents for combating various diseases, including Alzheimer's disease (AD). CADD employs structure-based drug design methodologies to investigate protein–ligand interactions, utilizing techniques such as molecular docking analysis, quantitative structure–activity relationship (QSAR) studies, and pharmacophore modeling [7, 8]. These approaches enable researchers to assess the binding affinity of drug candidates to target proteins, predict their pharmacological properties, and optimize their structure for improved efficacy and reduced toxicity. By providing a cost-effective and efficient means to explore potential drug candidates, CADD has become an invaluable tool in accelerating drug development [9, 10]. In the context of Alzheimer's disease, CADD is particularly instrumental in identifying and optimizing potent inhibitors that target key proteins involved in the disease process, with the goal of developing novel therapeutics with enhanced interactions and novel pharmacological profiles.

Galantamine, a natural compound used in the treatment of Alzheimer's disease and other memory-related disorders, exemplifies the potential of bioactive molecules derived from plants in therapeutic applications [11]. This alkaloid, predominantly sourced from species such as *Galanthus nivalis* (snowdrop), has a long history of use in traditional medicine for various ailments. As a cholinesterase inhibitor, galantamine works by increasing acetylcholine levels in the brain, thereby enhancing cholinergic neurotransmission, which is critical for learning and memory processes. Given its mechanism of action, galantamine has demonstrated efficacy in alleviating cognitive symptoms of AD, a progressive neurodegenerative disorder characterized by memory loss, impaired cognition, and behavioral changes [12]. Ongoing research continues to explore the potential of natural compounds, such as galantamine, in the development of novel AD therapies, with a particular focus on their ability to modulate key pathological processes underlying the disease.

Aristolochia indica, commonly referred to as Indian Birthwort or Ishwari, is a perennial herbaceous plant belonging to the Aristolochiaceae family. Native to the Indian subcontinent, it is widely distributed across various regions of Asia [13]. This plant has been extensively utilized in traditional medicinal systems, particularly in Ayurveda, owing to its purported therapeutic properties. However, its medicinal use warrants caution due to the presence of certain bioactive compounds with potential toxic effects. Given these safety concerns, evidence-based evaluation and expert consultation are essential before considering its medicinal application. The pharmacological significance of *A. indica* is attributed to its diverse array of biologically active constituents, some of which have been investigated for their therapeutic potential [14, 15]. Notably, molecular docking studies have emerged as a valuable tool for predicting the binding affinity of these compounds to specific biological targets. Our research aims to identify bioactive constituents of *A. indica* with high binding affinity through molecular docking analysis. Furthermore, their physicochemical characteristics and ADME (Absorption, Distribution, Metabolism, and Excretion) profiles. These investigations will focus on compounds exhibiting superior docking scores, with the objective of achieving enhanced target receptor interactions and potential pharmacological efficacy exceeding that of galantamine, a reference drug used in neurodegenerative disorders.

2 Materials and methods

2.1 Selection of protein target structure

Acetylcholinesterase (AChE) is a critical target for drug discovery, offering significant potential for identifying candidate therapeutic compounds. In this study, we employed the three-dimensional structures of human acetylcholinesterase (hAChE, PDB ID: 6O4 W) and *Torpedo californica* acetylcholinesterase (TcAChE, PDB ID: 1EVE), both retrieved from the Protein Data Bank (PDB) [16]. The hAChE protein comprises two chains (A and B), of which chain A was selected for molecular docking studies. To prepare the target proteins for docking, all water molecules and the bound donepezil ligand were removed. Subsequently, hydrogen atoms were added, bond orders were corrected, and Kollman charges were assigned to optimize the system. Since hydrogen atoms are frequently absent in crystallographic data, their inclusion was essential for accurate molecular interactions. The prepared protein structures were then converted to PDBQT format using Accelrys Discovery Studio and processed using AutoDock Vina [17, 18].

2.2 Preparation of ligand

The 3D structural data files (SDF) for the following natural compounds were obtained from the PubChem database and converted into PDB format using PyMol. The chemical structures of these natural compounds are shown in Fig. 1**.** The list

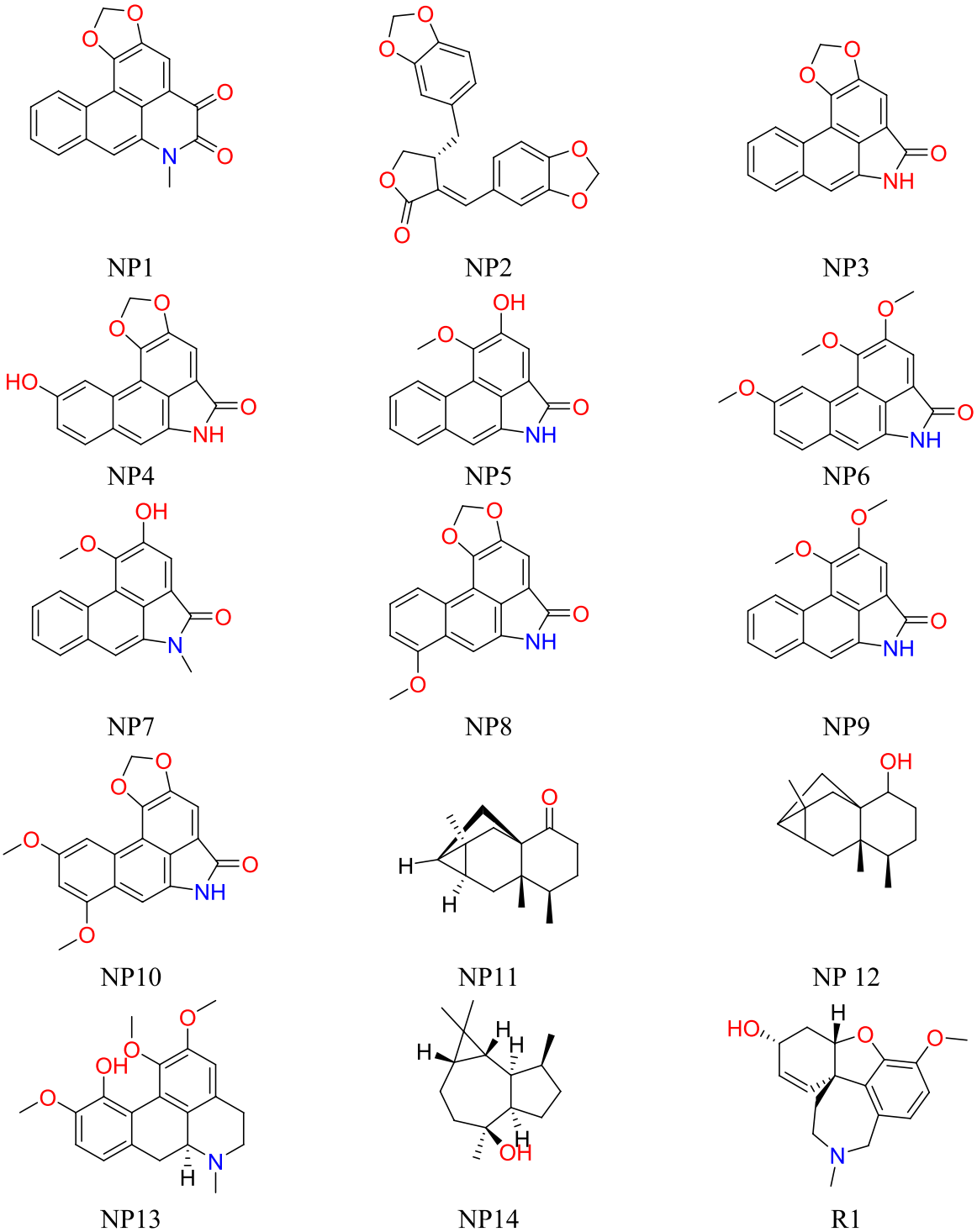


Fig. 1 Chemical structure of 14 Natural compounds (NP1-NP14) from *Aristolochia indica* plant and galantamine drug (R1)

comprises fourteen natural compounds, denoted as NP1 to NP14 (Cepharadione A (NP1), Savinin (NP2), Artistolactam II (NP3), Artistolactam IIIa (NP4), Artistolactam AII (NP5), Aristolactam B III (NP6), Sauristolactum (NP7), Artistolactam (NP8), Aristolactum BII (NP9), Artistolactam IV (NP10), Ishwarone (NP11), Ishwarol (NP12), Isocorydine (NP13), Ledol (NP14)) and along with a reference compound, Galantamine (R1).

2.3 Drug-likeness and ADME properties

Assessing the oral bioavailability of a compound is a critical step in drug discovery. Lipinski's rule of five serves as a widely accepted guideline for evaluating drug-like properties, stipulating that an orally active compound should meet the following criteria: (1) no more than five hydrogen bond donors, (2) no more than ten hydrogen bond acceptors, (3) a molecular weight below 500 Daltons (Da), and (4) an octanol–water partition coefficient (log P) of no more than five. In this study, these parameters were assessed using the MolSoft L.L.C. prediction tool. Computational methods play a pivotal role in predicting a compound's absorption, distribution, metabolism, excretion, and toxicity (ADMET) properties, significantly accelerating the drug development process while minimizing costs. The SwissADME online database provides a robust platform for evaluating these pharmacokinetic attributes in natural compounds. This computational approach enhances efficiency, conserves resources, and facilitates the identification of promising drug candidates with favorable safety and pharmacokinetic profiles [9, 19, 20].

2.4 Molecular docking studies

Molecular docking studies were performed to elucidate the mechanism of acetylcholinesterase (AChE) inhibition by natural compounds, assessing their binding affinities, interaction modes, and key molecular interactions with the target enzyme [21]. The three-dimensional structures of two AChE isoforms (PDB ID: 1EVE and 6O4 W) were retrieved from the Protein Data Bank (PDB) to serve as molecular targets. Docking simulations were conducted using AutoDock Vina 4.0, a widely employed open-source docking tool, to predict the binding conformations and stability of ligand-enzyme complexes. Prior to docking, the protein and ligand structures were prepared and converted into *pdbqt* format, ensuring compatibility with AutoDock Vina 4.0. Post-docking analyses, including binding energy estimations and interaction profiling, were carried out using Accelrys Discovery Studio, facilitating a comprehensive visualization of ligand–protein interactions, such as hydrogen bonding, hydrophobic contacts, and π-π stacking interactions. These insights provide a mechanistic understanding of how natural compounds modulate AChE activity, potentially guiding the development of novel inhibitors for neurodegenerative disorders [22–24].

2.5 Molecular dynamics (MD) simulations

Molecular dynamics (MD) simulations were performed using docked protein–ligand complexes as the baseline reference to assess the stability and dynamic behavior of interactions. As outlined in previous research by the authors, simulations were conducted using the GROMACS 2018.1 biomolecular software package, which is well-established for its accuracy in calculating non-bonded interactions, a critical aspect of molecular simulations [25, 26]. Ligand topologies were generated using the CHARMM General Force Field (CGenFF), while the CHARMM36 force field was employed for both ligand parameterization and protein structure preparation via the *pdb2 gmx* module. The system was subjected to an initial energy minimization step comprising 5,000 iterations using the steepest descent algorithm to eliminate steric clashes and stabilize atomic positions. A simulation box was constructed, maintaining a minimum distance of 10 Å between the protein–ligand complex and the box edges. The system was solvated using the TIP3P water model, and charge neutrality was ensured by adding Na^+ and Cl^- ions to attain a physiological salt concentration of 0.15 M. Equilibration was conducted in two phases: (i) a 100 ps NVT (constant volume and temperature) ensemble at 310 K using a modified Berendsen thermostat, followed by (ii) a 100 ps NPT (constant pressure and temperature) ensemble at 1 bar using the Parrinello-Rahman barostat to stabilize system pressure. The production run extended over 100 ns under physiological conditions. Trajectory analysis included root-mean-square deviation (RMSD) and root-mean-square fluctuation (RMSF) assessments to evaluate structural stability, and results were visualized using XMGRACE. These simulations provide critical insights into the conformational dynamics and binding stability of the studied protein–ligand complexes [27, 28].

2.6 Quantum chemical calculations

Computational analysis of key physicochemical properties was performed using the Gaussian 09 software package, employing the hybrid density functional theory (DFT) approach with the Lee–Yang–Parr functional and Becke's three-parameter exchange–correlation functional (B3LYP) in conjunction with the 6-311G(d,p) basis set. The study focused on

the evaluation of frontier molecular orbitals (FMOs), as these play a critical role in governing excitation-related properties and chemical reactivity. The highest occupied molecular orbital (HOMO) and lowest unoccupied molecular orbital (LUMO) energy levels were computed using the same theoretical framework to elucidate electronic properties and reactivity descriptors [29, 30]. Key parameters, including the HOMO–LUMO energy gap (ΔE), chemical hardness (η), softness (S), and chemical potential (μ), were derived based on the frontier orbital energies. This analysis adheres to the theoretical framework established by Parr and Pearson within the context of DFT and incorporates Koopmans'theorem, which establishes correlations between ionization potential (I), electron affinity (E), and the respective HOMO and LUMO energies (ε). These parameters provide valuable insights into the stability, reactivity, and electronic properties of the studied compounds, aiding in the prediction of their potential biological interactions and functional activity [31].

$$IP = -E_{HOMO} \quad EA = -E_{LUMO} \quad \mu = \frac{E_{HOMO} + E_{LUMO}}{2} \quad \eta = \frac{E_{HOMO} - E_{LUMO}}{2}$$

2.7 MM/GBSA calculations

The Molecular Mechanics/Generalized Born Surface Area (MM/GBSA) method is widely used to determine protein–ligand binding affinity across various systems and to estimate the binding free energy of ligands to macromolecules. In this study, the MM/GBSA calculations for the acetylcholinesterase–inhibitor complex were performed using the Prime module of Schrödinger's suite, as previously reported in the literature.

3 Results and discussion

3.1 Drug-likeness and ADME properties

In assessing drug-likeness, the molecular weight of the selected compounds falls within the range of 218 to 352 g/mol, aligning with established pharmacokinetic parameters for oral bioavailability. Several physicochemical properties play a crucial role in determining a compound's oral absorption and overall pharmacokinetic behavior, including lipophilicity, saturation, molecular size, flexibility, polarity, and solubility. The logarithm of the partition coefficient (LogP), a key determinant of lipophilicity, ranges from 1.84 to 5.0, indicating moderate to high permeability across biological membranes. The topological polar surface area (TPSA), which influences passive diffusion and interactions with transporters, varies between 17.07 and 71.55 $Å^2$. Optimal oral bioavailability is further supported by a restricted number of rotatable bonds (RB), ideally ranging from 0 to 3, ensuring conformational rigidity that facilitates efficient transport across lipid membranes. Additionally, hydrogen bond acceptors and donors, which influence solubility and receptor binding, fall within the optimal ranges of 1–5 and 0–2, respectively, as summarized in Table 1**.** The majority of these natural compounds conform to Lipinski's Rule of Five, a widely accepted criterion for drug-likeness, suggesting their potential for systemic bioavailability following oral administration.

Importantly, fourteen natural compounds demonstrated favorable gastrointestinal absorption, with a subset exhibiting the capacity to cross the blood–brain barrier **(**Table 2**).** This characteristic is particularly relevant for central nervous system (CNS)-targeted therapeutics, as it facilitates drug penetration into the brain parenchyma. However, the role of P-glycoprotein (P-gp), a crucial efflux transporter, must be considered in the pharmacokinetic profile of these compounds. P-gp plays a dual role: it restricts drug entry into the brain and epithelial cells lining the intestinal lumen, thereby modulating systemic exposure. Conversely, its contribution to drug excretion via hepatobiliary and renal pathways appears less pronounced. Additionally, P-gp has been implicated in the induction of drug-metabolizing enzymes, which may enhance drug clearance or, conversely, lead to increased drug-drug interactions and potential toxicity due to metabolic overload. A comprehensive evaluation of P-gp-mediated transport and metabolic activation is therefore essential in predicting the clinical viability of these compounds.

3.2 Molecular docking studies

Molecular docking studies demonstrated that the binding affinity of 14 natural compounds ranged from − 8.2 to − 11.2 kcal/mol with the 6O4 W protein, compared with the reference molecule, which exhibited a binding affinity of − 9.2 kcal/

Table 1 Drug-likeness molecules properties (NP1-NP14) and Galantamine (R1)

S. NO	MW (g/mol)	HBA	HBD	XLogP3	TPSA (Å)	RB
NP1	305.28	4	0	3.21	57.53	0
NP2	352.34	6	0	3.62	63.22	3
NP3	263.25	3	1	2.27	51.32	0
NP4	279.25	4	2	2.79	71.55	0
NP5	265.26	3	2	2.95	62.32	1
NP6	309.32	4	1	3.25	60.55	3
NP7	279.29	3	1	2.53	51.46	1
NP8	293.27	4	1	3.12	60.55	1
NP9	279.29	3	1	3.28	51.32	2
NP10	323.30	5	1	3.09	69.78	2
NP11	218.33	1	0	2.69	17.07	0
NP12	220.35	1	1	3.40	20.23	0
NP13	341.40	5	1	2.57	51.16	3
NP14	222.37	1	1	3.74	20.23	0
R1	287.35	4	1	1.84	41.93	1

MW Molecular Weight, *HBA* Hydrogen Bond Acceptor, *HBD* Hydrogen Bond Donator, *TPSA* Topological Polar Surface Area, *RB* Rotatable Bonds

Table 2 ADME Properties of natural compounds (NP1-NP14) and Reference drug (R1)

S.NO	GI abs	BBB	P-gp	CYP1 A2	CYP2 C19	CYP2 C9	CYP2D6	CYP3 A4	Log K_p
NP1	High	Yes	No	Yes	No	Yes	No	No	−5.88
NP2	High	Yes	No	Yes	Yes	Yes	Yes	Yes	−5.88
NP3	High	Yes	No	Yes	No	No	No	No	−5.67
NP4	High	Yes	No	Yes	No	No	Yes	No	−6.02
NP5	High	Yes	No	Yes	No	No	Yes	No	−5.82
NP6	High	Yes	No	Yes	Yes	Yes	Yes	Yes	−5.05
NP7	High	Yes	No	Yes	No	No	Yes	No	−5.78
NP8	High	Yes	No	Yes	No	Yes	Yes	Yes	−5.87
NP9	High	Yes	No	Yes	No	Yes	Yes	Yes	−5.67
NP10	High	Yes	No	Yes	No	Yes	Yes	Yes	−6.08
NP11	High	Yes	No	No	Yes	Yes	No	No	−5.44
NP12	High	Yes	No	No	Yes	Yes	No	No	−5.23
NP13	High	Yes	Yes	Yes	No	No	Yes	Yes	−6.56
NP14	High	Yes	No	No	Yes	No	No	No	−5.00
R1	High	Yes	Yes	No	No	No	Yes	No	−6.75

GI Gastrointestinal, *BBB* Blood–brain barrier, *P-gp* P-glycoprotein, *CYP* Cytochrome P

mol. Similarly, interactions with the 1EVE protein revealed binding affinities ranging from − 8.1 to − 11.2 kcal/mol for the natural compounds, whereas the reference molecule displayed a binding affinity of − 9.1 kcal/mol (Table 3). These findings suggest that several natural compounds exhibit comparable or superior binding interactions relative to the reference molecule, highlighting their potential as therapeutic candidates.

Molecular docking analysis demonstrated that NP1 exhibits high binding affinity and robust interactions with both human acetylcholinesterase (hAChE) and *Torpedo californica* acetylcholinesterase (TcAChE), suggesting its potential as a potent cholinesterase inhibitor. In hAChE, NP1 displayed a binding affinity of − 11.2 kcal/mol, forming 13 molecular interactions, including hydrogen bonding and multiple π interactions with key active site residues—TYR A:124, TYR A:133, TRP A:86, GLU A:202, TYR A:337, PHE A:338, and HIS A:447 **(**Fig. 2**).** In comparison, the reference drug galantamine exhibited a lower binding affinity of − 9.2 kcal/mol, establishing ten interactions, including hydrogen bonding with GLU A:202, π-π stacking and π-alkyl interactions with TRP A:86, carbon-hydrogen bonds with GLY A:121, and additional interactions with TYR A:337, TYR A:341, and HIS A:447 (Fig. 3). Similarly, docking studies against TcAChE revealed that NP1 exhibited a

Table 3 Molecular docking studies of selected natural compounds with reference compound on two varieties of acetylcholinesterase targets

S. No	PubChem CID	Natural compound Names	PDB ID: 6O4 W (Binding Affinity)	PDB ID: 1EVE (Binding Affinity)	Biological molecules
NP1	94,577	Cepharadione A	−11.2	−11.2	Isoquinoline alkaloid
NP2	5,281,867	Savinin	−11.0	−11.0	Benzodioxoles, a lignin
NP3	148,745	Aristolactam II	−11.0	−10.6	Aporphinoid alkaloids. phenanthrene
NP4	5,319,620	Aristololactam IIIa	−10.5	−10.9	Aporphinoid alkaloids. Phenanthrene
NP5	148,657	Aristolactam AII	−10.4	−10.5	Aporphinoid alkaloids. Phenanthrene
NP6	14,526,428	Aristolactam BIII	−10.5	−9.8	Aporphinoid alkaloids. Phenanthrene
NP7	131,002	Sauristolactam	−10.4	−9.2	Aporphinoid alkaloids. Phenanthrene
NP8	96,710	Aristololactam	−10.3	−10.3	Aporphinoid alkaloids. Phenanthrene
NP9	162,739	Aristolactam BII	−10.1	−10.1	Aporphinoid alkaloids. Phenanthrene
NP10	5,319,404	Aristololactam IV	−9.4	−10.3	Aporphinoid alkaloids. Phenanthrene
NP11	15,559,789	Ishwarone	−8.9	−9.0	tetracyclic sesquiterpene ketone
NP12	42,608,203	Ishwarol	−8.8	−8.7	Sesquiterpene
NP13	10,143	Isocorydine	−8.2	−8.7	quinoline alkaloids
NP14	11,074,994	Ledol	−7.9	−8.3	Sesquiterpenoid
R1		Galantamine	−9.2	−9.1	benzazepine alkaloid

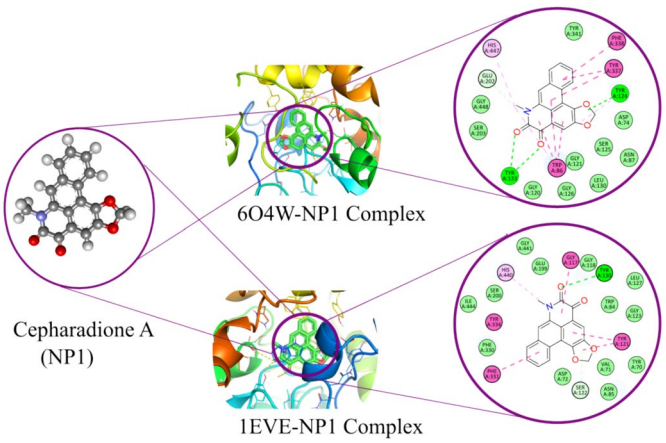


Fig. 2 Chemical Structure of Cepharadione A (NP1) and Its Interactions with hAChE and TcAChE Targets

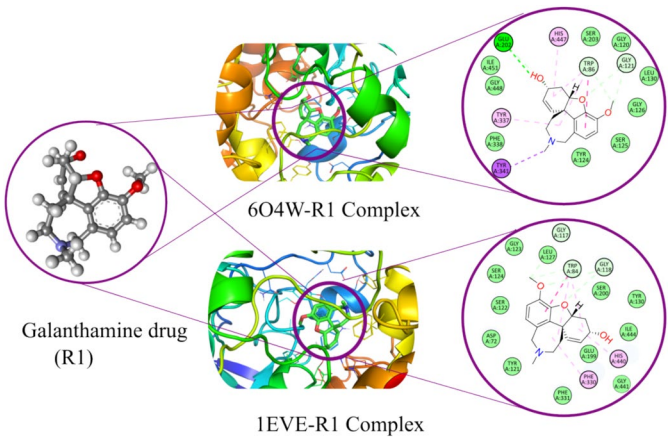


Fig. 3 Chemical Structure of Galantamine (R1) and Its Interactions with hAChE and TcAChE Targets

binding affinity of − 11.2 kcal/mol, forming eight interactions with critical residues, including TYR A:130, GLY A:117, TYR A:121, SER A:122, PHE A:331, TYR A:334, and HIS A:440 **(**Fig. 2**)**. In contrast, galantamine displayed a binding affinity of − 9.1 kcal/mol, engaging in nine molecular interactions, including π-alkyl, π-π stacking, and carbon-hydrogen bonds with TRP A:84, GLY A:117, GLY A:118, PHE A:330, and HIS A:440 (Fig. 3). The superior binding affinity and interaction stability of NP1 compared with galantamine suggest its enhanced inhibitory potential against both cholinesterase isoforms. These findings underscore the therapeutic relevance of NP1 in neurodegenerative disorders, particularly Alzheimer's disease, warranting further experimental validation through enzymatic and in vivo studies.

3.3 Molecular dynamics (MD) simulations

Computational analysis using Accelrys Discovery Studio demonstrated the successful convergence of NP1 and R1 ligand-protein complexes within hAChE (PDB ID: 6O4 W) and TcAChE (PDB ID: 1EVE) following a 100 ns molecular dynamics (MD) simulation. For the hAChE complex, root mean square deviation (RMSD) trajectories of the protein backbone exhibited an initial increase during the early frames, stabilizing at approximately 25 ns. Beyond this point, the RMSD values remained relatively constant until 80 ns. The average RMSD during the plateau phase (25–80 ns) was slightly lower for NP1 (0.15 ± 0.23 nm) compared with galantamine (0.15 ± 0.25 nm), suggesting a more stable and confined accommodation of NP1 within the hAChE binding site. Similarly, in the TcAChE complex, RMSD trajectories showed an initial rise, followed by stabilization around 5 ns, with a sustained plateau until 90 ns. The average RMSD during this phase (5–90 ns) was also slightly lower for NP1 (0.14 ± 0.28 nm) compared with galantamine (0.14 ± 0.33 nm), indicating greater structural stability of the NP1–TcAChE complex. However, RMSD values for NP1 and galantamine remained comparable over the entire 100 ns all-atom MD simulation. These findings collectively suggest that NP1 exhibits superior binding stability within both cholinesterase isoforms compared with galantamine, reinforcing its potential as a promising cholinesterase inhibitor for neurodegenerative disorders **(**Fig. 4**)**. The RMSF plots for both the protein and the ligand are presented in Fig. 5 and 6. Hydrogen bond analysis and protein–ligand contact histograms over a 100 ns simulation period for compound NP1 are shown in Fig. 7.

3.4 Quantum chemical calculations

Computational analysis revealed that NP1 and R1 exhibited the smallest HOMO–LUMO energy gaps, measuring 3.23 eV and 5.04 eV, respectively. These compounds also displayed the lowest chemical potentials, with values of −3.36 eV for NP1 and −5.60 eV for R1. Furthermore, NP1 and R1 demonstrated the highest chemical softness values among all analyzed compounds, recorded at 0.61 eV and 0.39 eV, respectively, suggesting enhanced chemical reactivity. In contrast, these compounds exhibited the lowest chemical hardness values, measured at 2.52 eV for NP1 and 1.67 eV for R1, indicating a higher susceptibility to chemical modifications **(**Table 4**,** Fig. 8**)**. These findings suggest that NP1 and R1

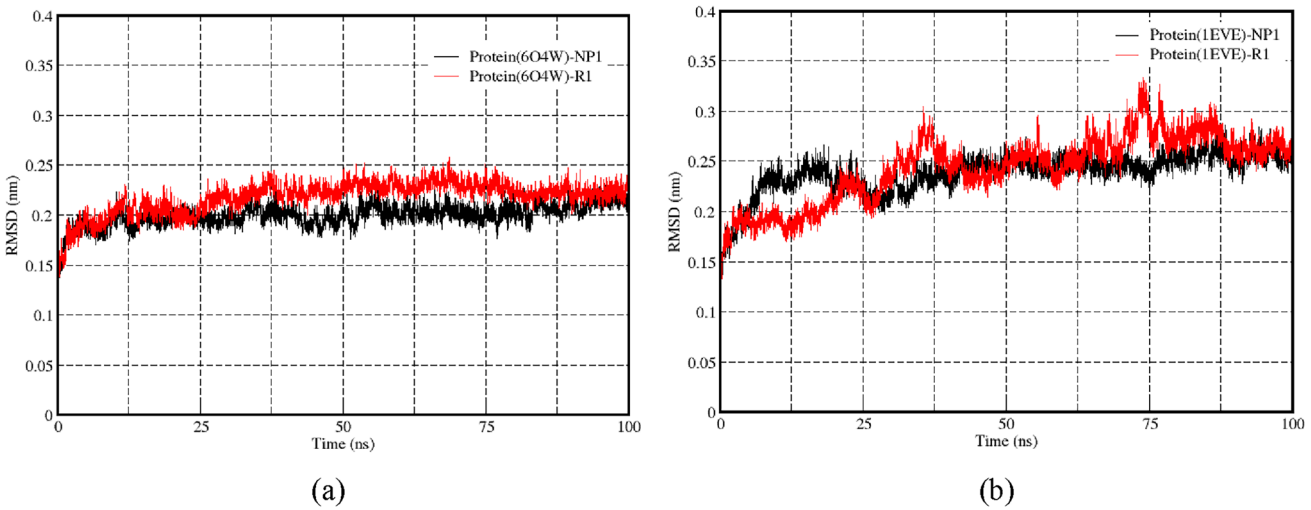


Fig. 4 (**a**) MD simulation for protein 1EVE with NP1, R1 complex stability, and (**b**) MD simulation for protein 6O4 W with NP1, R1 complex stability

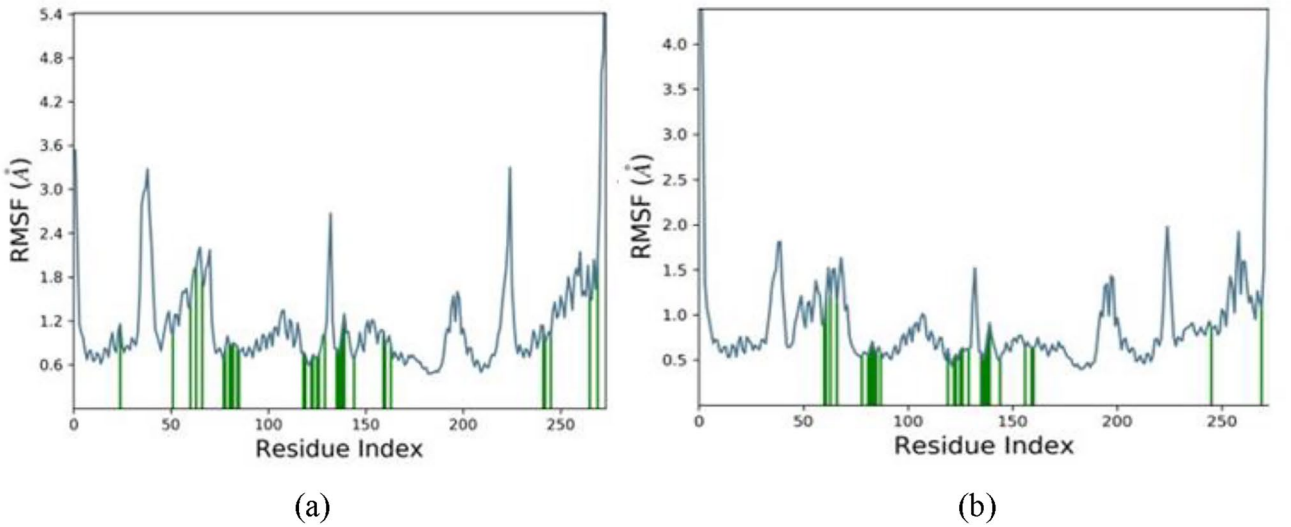


Fig. 5 Protein RMSF plots for (**a**) Protein IEVE and (**b**) 6O4 W

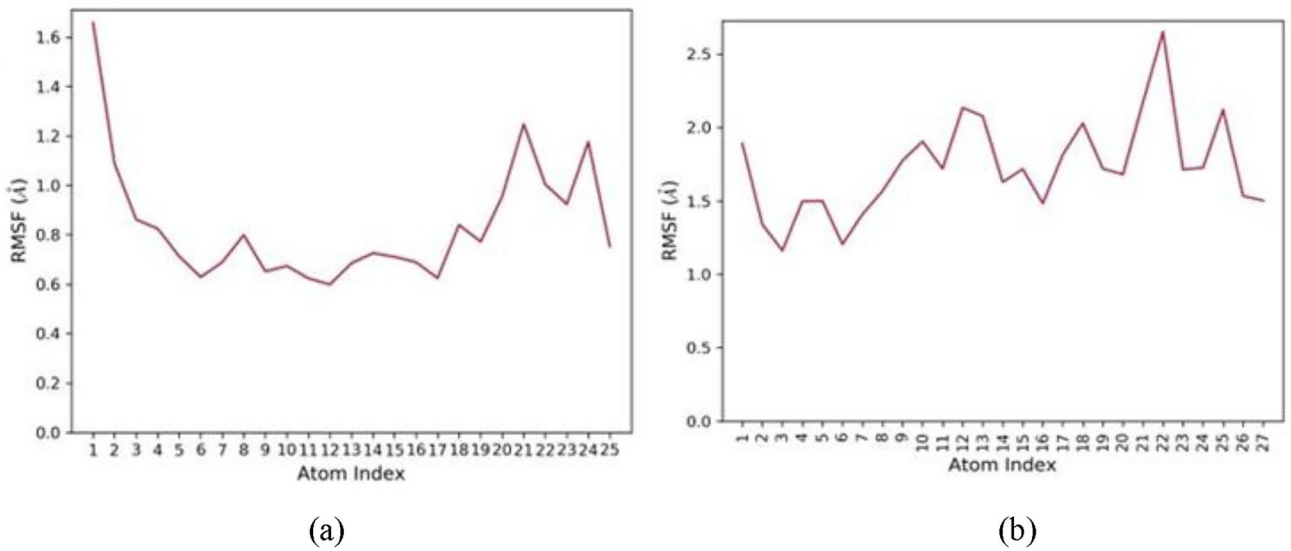


Fig. 6 Ligand RMSF plot for (**a**) NP1 and (**b**) R1

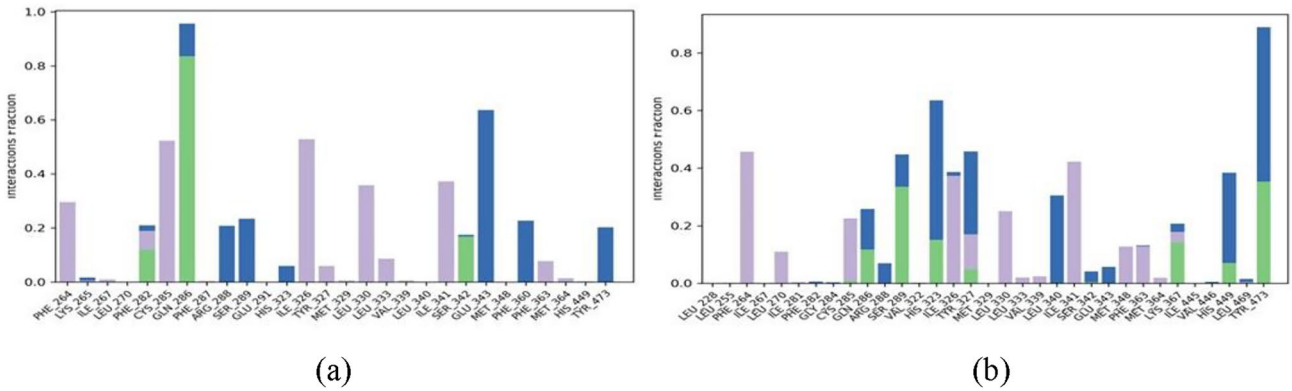


Fig. 7 Protein Ligand Contacts Histogram Over period of 100 ns compound NP1 (**a**) protein IEVE and (**b**) 6O4 W

Table 4 HOMO–LUMO Energies (eV), energy gap, hardness, softness, and chemical potential of NP1 and R1

Sr. No	HUMO (eV)	LUMO (eV)	IP	EA	Gap	Hardness	Softness	Chemical potential
NP 1	−2.65	−5.89	2.65	5.89	−3.23	1.67	0.61	−3.36
R1	−0.55	−5.60	0.55	5.60	−5.04	2.52	0.39	−5.60

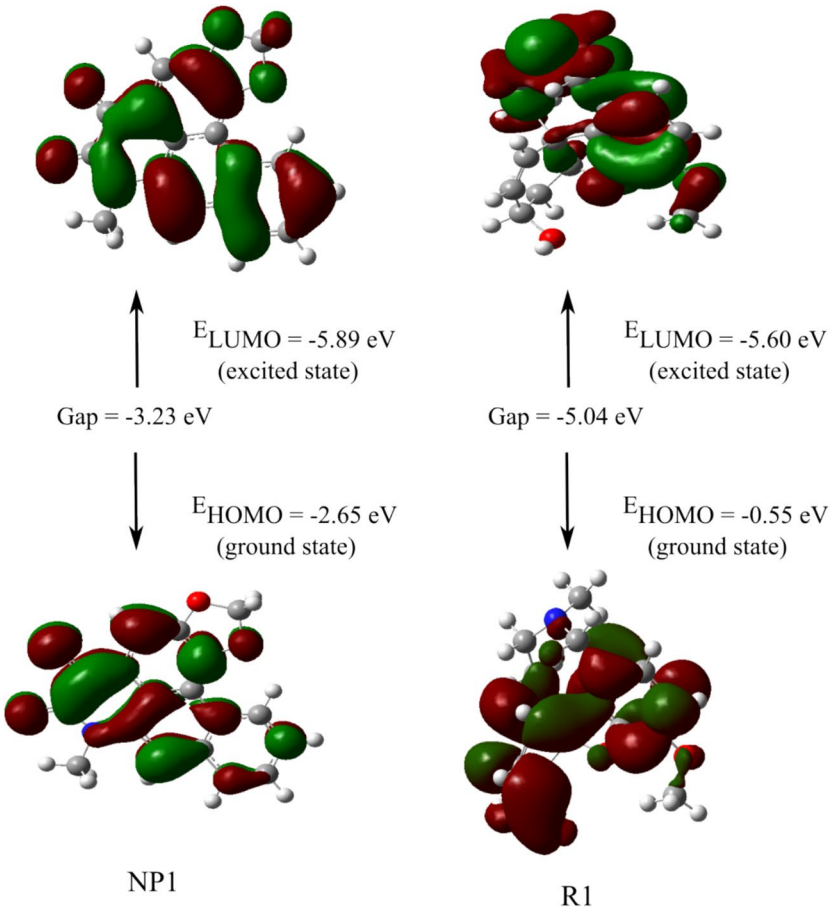


Fig. 8 HOMO–LUMO and energy gap of NP1 and R1 compounds

possess favorable electronic properties that may enhance their interaction with biological targets, warranting further experimental validation.

3.5 MM/GBSA calculations

To identify the thermodynamic and structural factors influencing the differential acetylcholinesterase inhibitory activity of NP1 and galantamine, Prime MM/GBSA calculations were performed. The Prime module, incorporating a local optimization feature, was utilized for energy minimization, with the OPLS4 force field and a continuum solvation model for GBSA. The binding free energy (ΔGbind) for each inhibitor within the acetylcholinesterase binding site was calculated using the appropriate equation, and the results are presented in Table 5.

4 Conclusion

This study utilized a computational approach to explore potential anti-Alzheimer's agents from a panel of 14 natural compounds, focusing on their interactions with human and *Torpedo* acetylcholinesterase (hAChE and TAChE). Among the screened compounds, NP1, isolated from *Aristolochia indica*, exhibited a higher binding affinity (−10.25 kcal/mol)

Table 5 MM/GBSA calculations of NP1 and galantamine

Compound	Prime energy Kcal/mol	Complex Energy Kcal/mol	MMGBSA dG Bind Kcal/mol	MMGBSA dG Bind Hbond Kcal/mol	MMGBSA dG Bind vdW Kcal/mol
NP1	−52.14	−10,882.4	−43.68	−1.42	−52.68
Galantamine	−48.36	−10,623.2	−40.23	−0.97	−50.21

than the reference inhibitor galantamine and outperformed NP2 (– 9.87 kcal/mol) and NP3 (– 8.92 kcal/mol). Molecular docking analysis revealed that NP1 formed stable hydrogen bonds with key active site residues, including ARG142 and GLU198. ADME profiling suggested NP1 adheres to Lipinski's Rule of Five, with a molecular weight of 312.27 Da, a logP of 2.95, and 2 hydrogen bond donors and 5 acceptors. It also showed high predicted gastrointestinal absorption (98.2%) and a favorable safety estimate (LD50 of 2800 mg/kg). MM-PBSA calculations supported these findings, with NP1 demonstrating a binding free energy of – 52.13 kcal/mol, which was lower than NP2 and NP3. Molecular dynamics simulations indicated stable binding of NP1 within the active site, with RMSD and RMSF values remaining below 1.5 Å. While these computational results are encouraging and position NP1 as a potential candidate for further investigation, experimental validation through in vitro and in vivo studies is necessary to substantiate its pharmacological potential and safety profile. Nonetheless, the lack of experimental data and blood–brain barrier permeability assessment limits the translational relevance of these findings.

Acknowledgements Srinivasarao Mande thanks the University of Hyderabad for the UGC non-NET fellowship and the Centre for Modelling Simulation and Design for computational facilities for conducting this research. I express my heartfelt appreciation to Shameer for his invaluable suggestions and assistance in expediting the article submission process.

Author contributions SM contributed to the creation of the abstract, gathered medical records for the case presentation, assisted in developing the discussion, and participated in the patient's care. LR was involved in drafting and researching the abstract, introduction, discussion, and conclusions. GNP was responsible for obtaining images for the article, HG: correcting errors in the case presentation, and took part in patient care. SG assisted in gathering information to develop the case, corrected errors in the discussion, and also participated in patient care. All authors reviewed and approved the final manuscript. KSG provided support in editing and proofreading the manuscript and gave final approval for its submission.

Funding This research was not funded by any public, commercial, or not-for-profit organizations.

Data availability The Data set generated during and/or unless during current study are available from the corresponding author on reasonable request.

Declarations

Ethics approval and consent of participate Not applicable.

Consent for publication Not applicable.

Competing interests The authors declare no competing interests.

Open Access This article is licensed under a Creative Commons Attribution 4.0 International License, which permits use, sharing, adaptation, distribution and reproduction in any medium or format, as long as you give appropriate credit to the original author(s) and the source, provide a link to the Creative Commons licence, and indicate if changes were made. The images or other third party material in this article are included in the article's Creative Commons licence, unless indicated otherwise in a credit line to the material. If material is not included in the article's Creative Commons licence and your intended use is not permitted by statutory regulation or exceeds the permitted use, you will need to obtain permission directly from the copyright holder. To view a copy of this licence, visit http://creativecommons.org/licenses/by/4.0/.

References

1. Karantzoulis S, Galvin JE. Distinguishing Alzheimer's disease from other major forms of dementia. Expert Rev Neurother. 2011;11(11):1579–91. https://doi.org/10.1586/ern.11.155.

2. Ismail Z, Smith EE, Geda Y, Sultzer D, Brodaty H, Smith G, Agüera-Ortiz L, Sweet R, Miller D, Lyketsos CG, Area IN. Neuropsychiatric symptoms as early manifestations of emergent dementia: provisional diagnostic criteria for mild behavioral impairment. Alzheimers Dement. 2016;12(2):195–202. https://doi.org/10.1016/j.jalz.2015.05.017.
3. Patočka J, Kuča K, Jun D. Acetylcholinesterase and butyrylcholinesterase–important enzymes of human body. Acta Medica (Hradec Kralove). 2004;47(4):215–28.
4. Rajagopalan V, Venkataraman S, Rajendran DS, Kumar VV, Kumar VV, Rangasamy G. Acetylcholinesterase biosensors for electrochemical detection of neurotoxic pesticides and acetylcholine neurotransmitter: a literature review. Environ Res. 2023;15(227): 115724. https://doi.org/10.1016/j.envres.2023.115724.
5. Akıncıoğlu H, Gülçin İ. Potent acetylcholinesterase inhibitors: potential drugs for Alzheimer's disease. Mini Rev Med Chem. 2020;20(8):703–15. https://doi.org/10.2174/1389557520666200103100521.
6. Walczak-Nowicka ŁJ, Herbet M. Acetylcholinesterase inhibitors in the treatment of neurodegenerative diseases and the role of acetylcholinesterase in their pathogenesis. Int J Mol Sci. 2021;22(17):9290. https://doi.org/10.3390/ijms22179290.
7. Mkhayar K, Elkhattabi K, Elkhalabi R, Haloui R, Daoui O, Edache EI, Chtita S, Elkhattabi S. Evaluation of dimedone-derived compounds as inhibitors against human colon cancer: Insights from 2D-QSAR, ADMET prediction, Osiris, Molinspiration, and molecular modeling. Chin J Anal Chem. 2023;51(11): 100330. https://doi.org/10.1016/j.cjac.2023.100330.
8. Edache EI, Uzairu A, Mamza PA, Shallangwa GA, Azam M, Min K. Methimazole and propylthiouracil design as a drug for anti-graves' disease: Structural studies, Hirshfeld surface analysis, DFT calculations, molecular docking, molecular dynamics simulations, and design as a drug for anti-graves' disease. J Mol Struct. 2023;5(1289): 135913. https://doi.org/10.1016/j.molstruc.2023.135913.
9. Ugbe FA, Shallangwa GA, Uzairu A, Abdulkadir I, Edache EI, Al-Megrin WA, Al-Shouli ST, Wang Y, Abdalla M. Cheminformatics-based discovery of new organoselenium compounds with potential for the treatment of cutaneous and visceral leishmaniasis. J Biomol Struct Dyn. 2024;42(24):13830–53. https://doi.org/10.1080/07391102.2023.2279269.
10. Edache EI, Uzairu A, Mamza PA, Shallangwa GA, Ibrahim MT. Evaluation of novel Anti-SARS-CoV-2 compounds by targeting nucleoprotein and envelope protein through homology modeling, docking simulations, ADMET, and molecular dynamic simulations with the MM/GBSA calculation. Intell Pharm. 2024;2(3):346–66. https://doi.org/10.1016/j.ipha.2024.02.008.
11. Sharma R, Kuca K, Nepovimova E, Kabra A, Rao MM, Prajapati PK. Traditional Ayurvedic and herbal remedies for Alzheimer's disease: from bench to bedside. Expert Rev Neurother. 2019;19(5):359–74. https://doi.org/10.1080/14737175.2019.1596803.
12. Heinrich M, Teoh HL. Galanthamine from snowdrop—the development of a modern drug against Alzheimer's disease from local Caucasian knowledge. J Ethnopharmacol. 2004;92(2–3):147–62. https://doi.org/10.1016/j.jep.2004.02.012.
13. Binorkar SV, Parlikar GR, Kulkarni AB. Bio-efficacy and Phyto-Pharmacological Activities of Aristolochia Indica Aristolochia Indica'nın biyoetkinliği ve fitofarmakolojik aktivitesi. Spatula DD. 2015. https://doi.org/10.5455/spatula.20151124064158.
14. Michl J, Jennings HM, Kite GC, Ingrouille MJ, Simmonds MS, Heinrich M. Is aristolochic acid nephropathy a widespread problem in developing countries?: A case study of Aristolochia indica L in Bangladesh using an ethnobotanical–phytochemical approach. J Ethnopharmacol. 2013;149(1):235–44. https://doi.org/10.1016/j.jep.2013.06.028.
15. Padhy GK. A review of Aristolochia indica: Ethnomedicinal uses, phytochemistry, pharmacological and toxicological effects. Curr Tradit Med. 2021;7(3):372–86. https://doi.org/10.2174/2215083806666200831173828.
16. Gerlits O, Ho KY, Cheng X, Blumenthal D, Taylor P, Kovalevsky A, Radić Z. A new crystal form of human acetylcholinesterase for exploratory room-temperature crystallography studies. Chem Biol Interact. 2019;25(309): 108698. https://doi.org/10.1016/j.cbi.2019.06.011.
17. Gudasi S, Gharge S, Koli R, Patil K. Antioxidant properties and cytotoxic effects of Oxalis corniculata on human Hepatocarcinoma (Hep-G2) cell line: an in vitro and in silico evaluation. Futur J Pharm Sci. 2023;9(1):25. https://doi.org/10.1186/s43094-023-00476-2.
18. Gudasi S, Gharge S, Koli R, Kagawad P. Exploring in-silico, in-vitro antioxidant, and cytotoxic potential of valerian wallichii by on cervical epithelial carcinoma (HeLa) cell lines. Chem Biodivers. 2024;21(3): e202302072. https://doi.org/10.1002/cbdv.202302072.
19. Edache EI, Uzairu A, Shallangwa GA, Mamza PA. Virtual screening, pharmacokinetics, and molecular dynamics simulations studies to identify potent approved drugs for Chlamydia trachomatis treatment. Futur J Pharm Sci. 2021;7:1–22. https://doi.org/10.1186/s43094-021-00367-4.
20. Ugbe FA, Shallangwa GA, Uzairu A, Abdulkadir I. Computational design, molecular properties, ADME, and toxicological analysis of substituted 2, 6-diarylidene cyclohexanone analogs as potent pyridoxal kinase inhibitors. In Silico Pharm. 2023;11(1):6. https://doi.org/10.1007/s40203-023-00142-8.
21. Singh KD, Kirubakaran P, Nagarajan S, Sakkiah S, Muthusamy K, Velmurgan D, Jeyakanthan J. Homology modeling, molecular dynamics, e-pharmacophore mapping and docking study of Chikungunya virus nsP2 protease. J Mol Model. 2012;18:39–51. https://doi.org/10.1007/s00894-011-1018-3.
22. Ugbe FA, Edache EI, Ayuba AM, Ibrahim MT, Umar AB, Adeniji SE, Abdalla M, Al-Megrin WA, Eltayeb LB, Thagfan FA, Albutti A. Cheminformatic evaluation of the multi-protein binding potential of some diselenide derivatives: a plausible drug discovery approach for leishmaniasis. Discov Chem. 2024;1(1):25. https://doi.org/10.1007/s44371-024-00026-6.
23. Edache EI, Uzairu A, Mamza PA, Shallangwa GA, Ibrahim MT. Towards designing of some potential new autoimmune disorder inhibitors using crystal structures and Hirshfeld surface analyses in combination with molecular docking and molecular dynamics simulations. Intell Pharm. 2024;2(2):204–25. https://doi.org/10.1016/j.ipha.2023.11.008.
24. Ugbe FA, Shallangwa GA, Uzairu A, Abdulkadir I. Molecular docking investigation, pharmacokinetic analysis, and molecular dynamic simulation of some benzoxaborole-benzimidazole hybrids: an approach to identifying superior onchocerca inhibitors. Borneo J Pharm. 2023;6(1):58–78.
25. Ugbe FA, Edache EI, Adeniji SE, Arthur DE, Ajala A, Adawara SN, Ejeh S, Ibrahim ZY. Computational evaluation of the inhibitory potential of some urea, thiourea, and selenourea derivatives of diselenides against leishmaniasis: 2D-QSAR, pharmacokinetics, molecular docking, and molecular dynamics simulation. J Mol Struct. 2024;15(1302): 137473. https://doi.org/10.1016/j.molstruc.2023.137473.
26. Gharge S, Alegaon SG, Ranade SD, Khatib NA, Kavalapure RS, Kumar BP, Vinod D, Bavage NB. Design, synthesis of new 2, 4-thiazolidinediones: In-silico, in-vivo anti-diabetic and anti-inflammatory evaluation. Eur J Med Chem Rep. 2024;1(11): 100151. https://doi.org/10.1016/j.ejmcr.2024.100151.

27. Gharge S, Alegaon SG, Jadhav S, Ranade SD, Kavalapure RS. Design, synthesis, characterization and antidiabetic evaluation of 3, 5-substituted thiazolidinediones: evidenced by network pharmacology, molecular docking, dynamic simulation, in vitro and in vivo assessment. Eur J Med Chem Rep. 2024;1(12): 100213. https://doi.org/10.1016/j.ejmcr.2024.100213.
28. Ranade SD, Alegaon SG, Khatib NA, Gharge S, Kavalapure RS, Kumar BP. Design, synthesis, molecular dynamic simulation, DFT analysis, computational pharmacology and decoding the antidiabetic molecular mechanism of sulphonamide-thiazolidin-4-one hybrids. J Mol Struct. 2024;5(1311): 138359. https://doi.org/10.1016/j.molstruc.2024.138359.
29. Ugbe FA, Shallangwa GA, Uzairu A, Abdulkadir I. Molecular docking screening and pharmacokinetic studies of some boron-pleuromutilin analogues against possible targets of wolbachia pipientis. J Mol Docking. 2022;2(1):29–43.
30. Gharge S, Alegaon SG, Ranade SD, Kavalapure RS, Kumar BP. Novel rhodanine–thiazole hybrids as potential antidiabetic agents: a structure-based drug design approach. RSC Med Chem. 2025. https://doi.org/10.1039/D4MD00689E.
31. Gharge S, Alegaon SG, Ranade SD, Kavalapure RS, Kumar BP, Mhaske PC. Expression of PPAR-γ TF by newly synthesized thiazolidine-2, 4-diones to manage glycemic control: Insights from in silico, in vitro and experimental pharmacology in wistar rats. Bioorg Chem. 2024;1(153): 107966. https://doi.org/10.1016/j.bioorg.2024.107966.

Publisher's Note Springer Nature remains neutral with regard to jurisdictional claims in published maps and institutional affiliations.